

LA-UR- 96-4068

CONF-961202--30

Title:

SITE OCCUPANCIES IN TERNARY CIS ORDERED LAVES PHASES

Author(s):

Paul G. Kotula, CMS  
Ian M. Anderson, ORNL  
Fuming (NMI) Chu, CMS  
Daniel J. Thoma, MST-6 J  
ames (NMI) Bentley, ORNL  
Terence E. Mitchell, CMS

DEC 26 1996

OSTI

Submitted to:

Fall 1996 MRS Meeting  
Boston MA

December 2-6, 1996

MASTER

**Los Alamos**  
NATIONAL LABORATORY

Los Alamos National Laboratory, an affirmative action/equal opportunity employer, is operated by the University of California for the U.S. Department of Energy under contract W-7405-ENG-36. By acceptance of this article, the publisher recognizes that the U.S. Government retains a nonexclusive, royalty-free license to publish or reproduce the published form of this contribution, or to allow others to do so, for U.S. Government purposes. The Los Alamos National Laboratory requests that the publisher identify this article as work performed under the auspices of the U.S. Department of Energy.

*dy*  
DISTRIBUTION OF THIS DOCUMENT IS UNLIMITED

Form No. 836 R5  
ST 2629 10/91

#### **DISCLAIMER**

**Portions of this document may be illegible  
in electronic image products. Images are  
produced from the best available original  
document.**

# SITE OCCUPANCIES IN TERNARY C15 ORDERED LAVES PHASES

PAUL G. KOTULA\*, IAN M. ANDERSON\*\*, FUMING CHU\*, DAN J. THOMA\*,  
JIM BENTLEY\*\*, AND TERENCE E. MITCHELL\*

\* Materials Science and Technology Division, Mail Stop K765, Los Alamos National Laboratory,  
Los Alamos, NM 87545

\*\*Metals and Ceramics Division, Oak Ridge National Laboratory, P O Box 2008, Oak Ridge, TN  
37831

## ABSTRACT

Site occupancies in three C15-structured  $AB_2(X)$  Laves phases have been determined by Atom Location by CHanneling Enhanced Microanalysis (ALCHEMI). In  $NbCr_2(V)$ , the results were consistent with exclusive site occupancies of Nb for the A sublattice and Cr and V for the B sublattice. The B-site occupancy of V is not expected from atom size effects alone. In  $NbCr_2(Ti)$ , the results were consistent with Ti partitioning mostly to the A sites with some anti-site defects likely. In  $HfV_2(Nb)$ , the results were consistent with Nb partitioning between the A and B sites. The results of the ALCHEMI analyses of these ternary C15 Laves phase materials will be discussed with respect to previously determined phase diagrams and first-principles total energy and electronic structure calculations.

## INTRODUCTION

Laves-phase intermetallics are of potential use as high-temperature structural materials,<sup>1-8</sup> superconductors<sup>9,10</sup> and hydrogen storage materials.<sup>11</sup>  $NbCr_2$ -based and  $HfV_2$ -based C15 structured alloys are of interest for such applications.<sup>4</sup> The defect mechanism of a ternary Laves phase is crucial to understanding its physical metallurgy and deformation behavior.<sup>5</sup> Three different alloy systems have therefore been chosen for this study:  $NbCrV$ ;  $NbCrTi$ ; and  $HfVNb$ . Vanadium-alloyed  $NbCr_2$  Laves phase materials have been studied previously.<sup>12</sup> It is suggested based on the  $Nb$ - $Cr$ - $V$  phase diagram and first-principles total energy and electronic structure calculations for  $NbCr_2$  that V should occupy the B sites in C15-structured  $AB_2$ .<sup>12</sup> From a similar set of arguments, it is expected for Nb-alloyed  $HfV_2$  that there should be no site preference for Nb.<sup>13</sup> In this paper, ALCHEMI<sup>14</sup> is employed to examine the site occupancies of ternary alloy additions to C15 Laves phase materials.

## EXPERIMENTAL

Alloys of composition  $Nb_{33}Cr_{42}V_{25}$ ,  $Nb_{10}Cr_{75}Ti_{15}$ ,  $Nb_{20}Cr_{60}Ti_{20}$  and  $Hf_{25}V_{60}Nb_{15}$  were prepared by arc-melting followed by annealing at 1400°C (1200°C for the Hf alloy) for 120 h. Specimens were prepared for microanalysis by cutting 3 mm discs followed by dimpling and ion milling. Energy-dispersive x-ray (EDX) spectra were acquired near  $\langle 014 \rangle$  over a range of  $\{400\}$  excitations between symmetry and beyond  $\{12\ 0\ 0\}$ . Spectra were also acquired near  $\langle 334 \rangle$  over a range of  $\{440\}$  excitations between symmetry and  $\{880\}$ . A Philips CM30 operating at 300 kV equipped with a Kevex Quantum detector, a Philips CM12 operating at 120 kV and equipped with an EDAX superUTW detector and a Philips CM200 FEG equipped with a Link detector were all utilized for the present study. Site-distributions were extracted from the data by multivariate statistical analysis (MSA)<sup>15</sup> with delocalization correction<sup>16</sup> as described elsewhere.<sup>17,18</sup>

## RESULTS AND DISCUSSION

The C15 Laves phase structure is essentially the same as the oxide spinel structure without oxygen. Therefore, for the compound  $AB_2$  ( $NbCr_2$  or  $HfV_2$  in this case) there are two distinct sublattices: A (the tetrahedral site in spinel) and B (the octahedral site in spinel). Figure 1 shows X-ray spectra collected at {800} under conditions that maximized the electron fluence on the A and B sublattices. The correlated variation of the V and Cr characteristic X-ray peaks gives qualitative evidence of similar site-distributions for these elements. However, the precision of the site-distribution extracted with MSA was poor. This imprecision can be explained by the similarity of the variations of all X-rays to the channeling, as shown in Figure 2. Although the variation of the  $Nb\text{ K}\alpha$  intensity is opposite to those of the V and Cr  $K\alpha$  intensities, the shapes of the three curves are similar. The three curves do not therefore vary independently, as required by MSA. The lack of site-discrimination at {800} can be attributed to the similar elastic scattering powers of the alternating planes, of composition Nb and  $Cr_2$  in the stoichiometric binary alloy. Indeed, the intensity of the 400 reflection was relatively weak. ALCHEMI was therefore performed at the {440} systematic row, with alternating planes of composition NbCr and Cr. Here, the intensity of the 220 reflection, due entirely to scattering from the A sublattice, was pronounced. Figure 3 shows the variation of the delocalization-corrected intensity ratios<sup>18</sup> with orientation. The correction coefficients  $L_{CrX}$  were all within 2% of unity for the medium energy X-rays used for quantification. In contrast to the data in Fig. 2, the signals for the two host elements vary independently of one another. MSA indicated a  $99.3 \pm 3.9\%$  correlation between V and Cr. The relatively large statistical error arises because the two sublattices are not completely separated onto alternating planes at {440}.<sup>18</sup> However, the result is consistent with exclusive site-occupancies of Nb for the A sublattice and Cr and V for the B sublattice.

In the C15 structure, the ideal ratio of atomic radii for the A and B sites is  $\sqrt{3/2} \approx 1.225$  although ratios of ~1.1 to 1.6 are observed. In binary  $NbCr_2$ , the ratio of the Nb (2.08 Å) to Cr (1.85 Å) radii is ~1.13. It is expected from size effects that V (1.92 Å) would substitute for Nb on the A sublattice. As the V is found to substitute for Cr, it is clear that electronic effects must be more important than size effects in this case. First-principles total energy and electronic structure calculations suggest that V addition to  $NbCr_2$  should stabilize the C15 structure by lowering the fermi level to between the bonding and antibonding states of the total density of states.<sup>12</sup> Indeed it is seen from the  $NbCrV$  phase diagram that the C15 phase field is elongated parallel to the Cr-V edge of the diagram out to 30 at.-% V, indicating that V solely occupies Cr sites and V serves to stabilize the C15 structure.<sup>12</sup>

Figure 4 shows the variation of the delocalization-corrected intensity ratios with orientation for  $Nb_{10}Cr_{7.5}Ti_{15}$ . MSA indicated a  $91.1 \pm 1.6\%$  correlation between Nb and Ti. In this case, the results are consistent with all of the Ti occupying the A sublattice (i.e.,  $TiCr_2$ ) with the Nb partitioning between the A and B sites. This alloy consisted of three phases: C15 Laves phase  $Nb_{14}Cr_{6.9}Ti_{17}$  (64%); Cr-rich bcc solid-solution  $Cr_{9.3}Ti_7$  (35%); and a Ti phase (2%). Assuming no anti-site defects (i.e., of Ti and Cr with each other) this gives  $(Ti_{17}Nb_{13})_A[Cr_{6.9}Nb_1]_B$  for the Laves phase. Clearly this formulation would require some anti-site defects to maintain stoichiometry.

The variation of the delocalization-corrected intensity ratios with orientation for  $Nb_{20}Cr_{6.0}Ti_{20}$  is shown in Figure 5. MSA indicated an  $80.2 \pm 2.0\%$  correlation between Ti and Nb. The results are consistent with all of the Nb occupying the A sublattice with Ti, in this case, partitioning between the sites. This particular alloy had approximately 5% of a second phase (predominantly Ti). The composition of the Laves phase was determined to be approximately  $Nb_{21}Cr_{6.3}Ti_{16}$ . Assuming no anti-site defects (i.e., of Nb or Cr with each other), this corresponds, for the Laves phase, to:  $(Nb_{21}Ti_{13})_A[Cr_{6.3}Ti_3]_B$ . For both NbCrTi alloys, the Nb and Ti had a decided preference for the A-site but

The results of ALCHEMI on the  $HfVNb$  alloy are given in Figure 6. MSA indicated a  $54.0 \pm 9.4\%$  correlation between Nb and V. Assuming that there are no anti-site defects (i.e., of Hf or V), the results are consistent with the Nb occupying both lattice sites with a slight preference for

the Hf-site. First-principles total energy and electronic structure calculations suggest that there should be no preference of Nb for either sublattice.<sup>13</sup> Additionally, x-ray diffraction experiments are in agreement with the ALCHEMI findings.<sup>13</sup>

## CONCLUSIONS

Site occupancies for ternary alloying additions to C15-structured Laves phase materials have been determined with ALCHEMI. As illustrated in the above examples, there are a number of different point defect mechanisms/structures possible in ternary Laves phase materials. Atom-size effects may not be the dominant factor for determining the stability of Laves phase materials. As shown for the NbCrV system, electronic effects may also play a role.<sup>12</sup> V substitutes exclusively for Cr which is not predicted by the atomic size rules. In the NbCrTi system the apparent point-defect behavior varies with composition, in one case behaving like TiCr<sub>2</sub> with Nb additions (Nb<sub>1.0</sub>Cr<sub>7.5</sub>Ti<sub>1.5</sub>) and in the other like NbCr<sub>2</sub> with Ti additions (Nb<sub>2.0</sub>Cr<sub>6.0</sub>Ti<sub>2.0</sub>). Clearly more work is required in order to fully understand the point defect behavior of this ternary system. In both cases though, partitioning of the 'alloying addition' occurs with Ti and Nb, occupying the A site predominantly. In the HfVNb system there is a slight site preference of Nb for the Hf site in HfV<sub>2</sub>-based C15 Laves phase. This is consistent with theoretical calculations for this system.<sup>13</sup>

## ACKNOWLEDGMENTS

Research at Los Alamos National Laboratory (LANL) was sponsored by the US Department of Energy (DOE)-OBES. Research at Oak Ridge National Laboratory (ORNL) SHaRE User Facility was sponsored by the DOE Division of Materials Sciences under contract DE-AC05-96OR22464 with Lockheed Martin Energy Research Corp. and by an appointment (IMA) to the ORNL Postdoctoral Research Associates Program, which is administered jointly by the Oak Ridge Institute for Science and Education and ORNL. PGK acknowledges a Director-funded postdoctoral fellowship from LANL.

## REFERENCES

1. J. D. Livingston and E. L. Hall, *J. Mater. Res.* **5** (1) (1990) 5.
2. R. L. Fleischer and R. J. Zabala, *Met. Trans. A* **21A** (1990) 2149.
3. M. Takeyama and C. T. Liu, *Mater. Sci. Eng.* **A132** (1991) 61.
4. D. J. Thoma and J. H. Perepezko, *Mater. Sci. Eng.* **A156** (1992) 97.
5. F. Chu and D. P. Pope, *Mater. Sci. Eng.* **A170**, (1993) 39.
6. K. S. Kumar and D. B. Miracle, *Intermetallics* **2**, (1994), 257-274.
7. G. E. Vignoul, J. K. Tien, and J. M. Sanchez, *Mater. Sci. Eng.* **A170**, (1993) 177.
8. T. Takasugi, M. Yoshida, and S. Hanada, *Acta Met. et Mater.* (1995).
9. S. V. Vonsovsky, Y. A. Izyumov, and E. Z. Kurmaev, *Superconductivity of Transition Metals*, Springer-Verlag, Berlin, 1982.
10. F. Chu, Z. W. Chen, C. J. Fuller, C. L. Lin, and T. Mihalisin, *J. Appl. Phys.* **79**(8) (1996), 6405.
11. K. Aoki, X.-G. Li and T. Masumoto, *Acta Metall. et Mater.* **40**(2) (1992) 221.
12. F. Chu, D. J. Thoma, P. G. Kotula, S. Gerstl, and T. E. Mitchell, in preparation.
13. F. Chu, D. P. Pope, D. J. Thoma, Y. C. Lu, P. G. Kotula and T. E. Mitchell, in preparation.
14. J. C. H. Spence and J. Taftø, *J. Microscopy* **130**(1983)147.
15. C. J. Rossouw et al., *Phil. Mag. Lett.* **60**(1989)225.
16. M. G. Walls, *Microsc. Microanal. Microstruct.* **3**(1992)443.
17. I. M. Anderson and J. Bentley, *Proc. 13th ICEM: Electron Microscopy 1994* 1(1994)609.
18. I. M. Anderson and J. Bentley, *Proc. EMAG 95. Bristol: Inst. of Physics* (1996).

## FIGURES

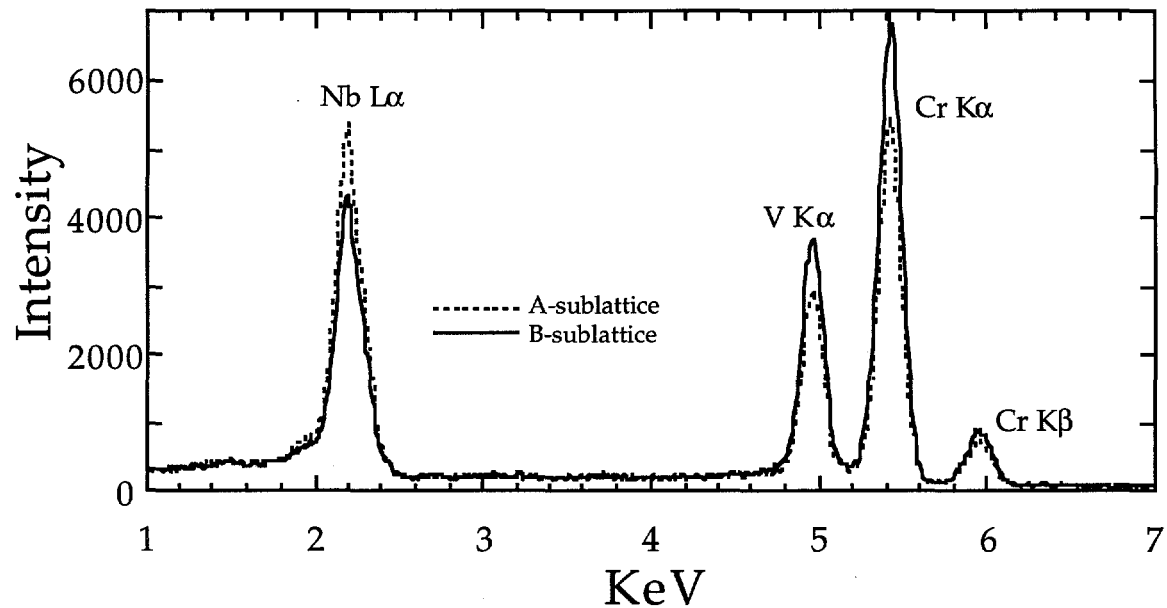


Fig. 1. EDX spectra acquired at {800} with electron fluence on the A and B sublattices.

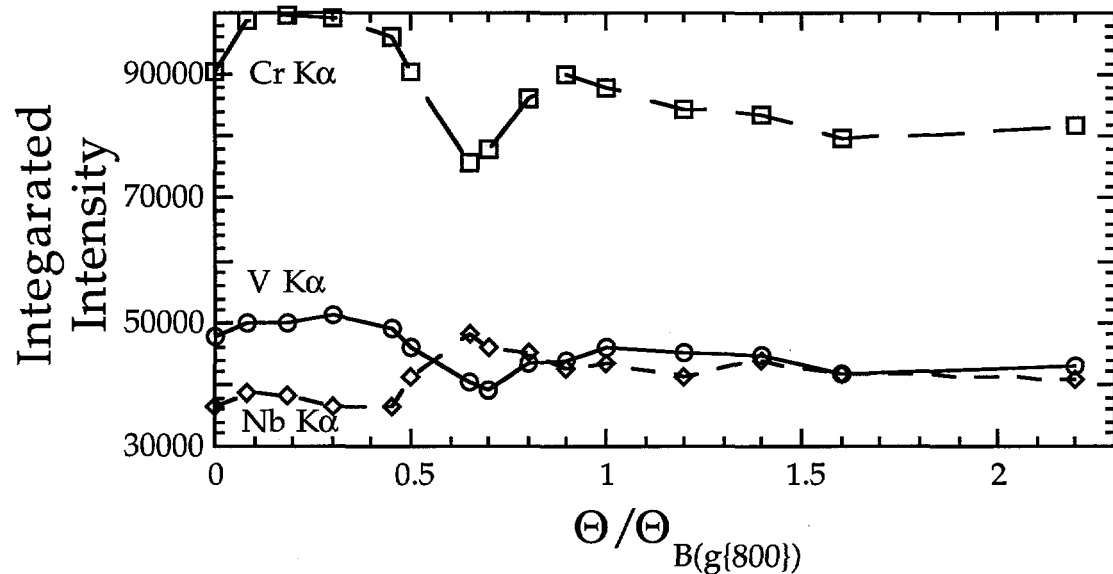


Fig. 2. Variation of integrated X-ray intensities with orientation at the {800} systematic row.

## DISCLAIMER

This report was prepared as an account of work sponsored by an agency of the United States Government. Neither the United States Government nor any agency thereof, nor any of their employees, makes any warranty, express or implied, or assumes any legal liability or responsibility for the accuracy, completeness, or usefulness of any information, apparatus, product, or process disclosed, or represents that its use would not infringe privately owned rights. Reference herein to any specific commercial product, process, or service by trade name, trademark, manufacturer, or otherwise does not necessarily constitute or imply its endorsement, recommendation, or favoring by the United States Government or any agency thereof. The views and opinions of authors expressed herein do not necessarily state or reflect those of the United States Government or any agency thereof.

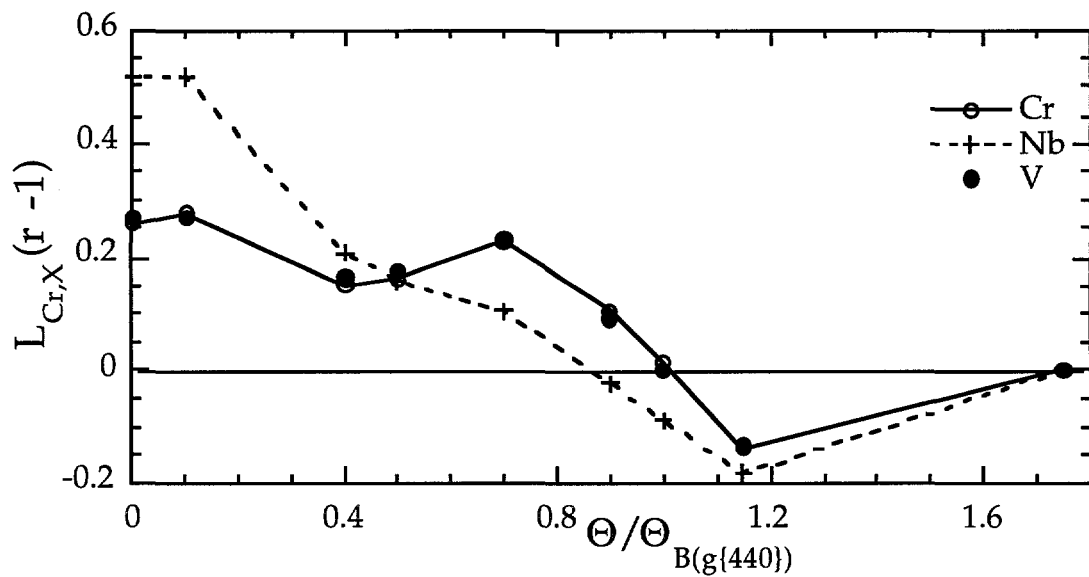


Fig. 3. Variation of delocalization-corrected intensity ratios of  $Nb_{33}Cr_{42}V_{25}$  with orientation at the  $\{440\}$  systematic row.

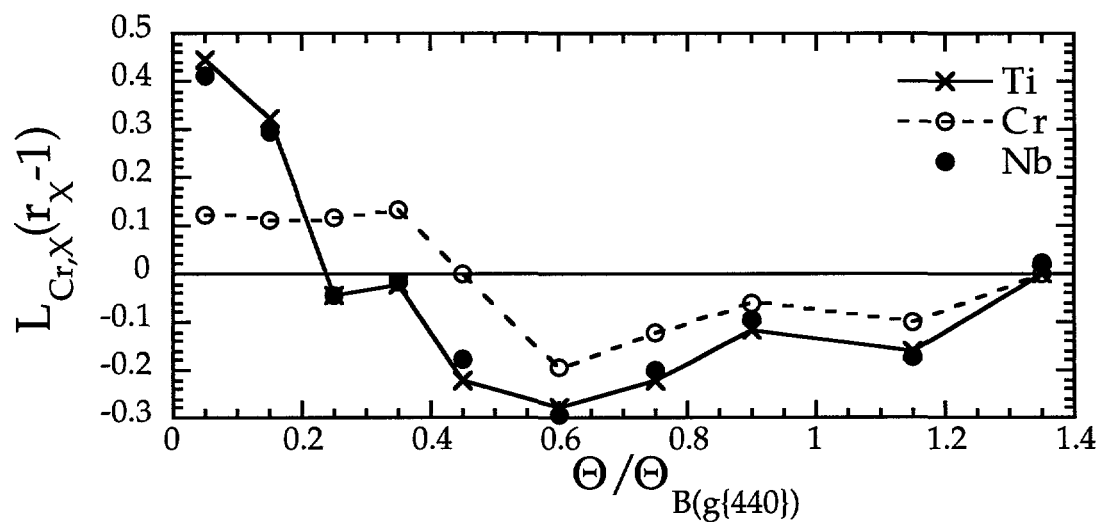


Fig. 4. Variation of delocalization-corrected intensity ratios of  $Nb_{10}Cr_{75}Ti_{15}$  with orientation at the  $\{440\}$  systematic row.

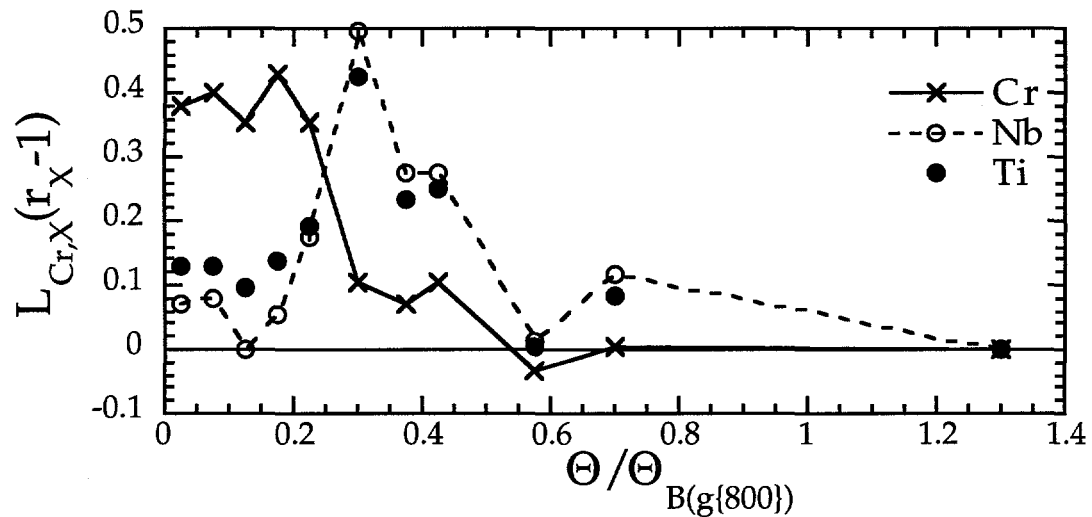


Fig. 5. Variation of delocalization-corrected intensity ratios of  $\text{Nb}_{20}\text{Cr}_{60}\text{Ti}_{20}$  with orientation at the  $\{800\}$  systematic row.

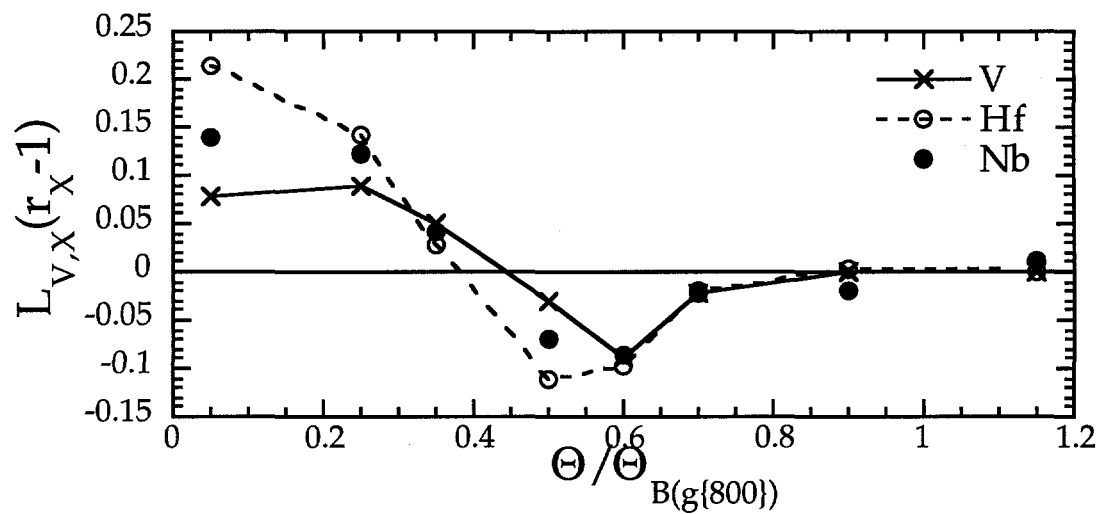


Fig. 6. Variation of delocalization-corrected intensity ratios of  $\text{Nb}_{20}\text{Cr}_{60}\text{Ti}_{20}$  with orientation at the  $\{800\}$  systematic row.